

3D ELECTROMAGNETIC AND BEAM DYNAMICS MODELING OF THE LANSCE DRIFT-TUBE LINAC

S.S. Kurennoy and Y.K. Batygin, LANL, Los Alamos, NM 87545, USA

Abstract

The LANSCE drift-tube linac (DTL) accelerates the proton or H^- beam to 100 MeV. It consists of four tanks containing tens of drift tubes and post-couplers; for example, tank 2 is almost 20 m long and has 66 cells. We have developed 3D models of full tanks [1] in the DTL with CST Studio to accurately calculate the tank modes, their sensitivity to post-coupler positions and tilts, tuner effects, and RF-coupler influence. Electromagnetic analysis of the DTL tank models is performed using MicroWave Studio (MWS). The full-tank analysis allows tuning the field profile of the operating mode and adjusting the frequencies of the neighboring modes within a realistic CST model. Beam dynamics is modeled with Particle Studio for bunch trains with realistic initial beam distributions using the MWS-calculated and tuned RF fields and quadrupole magnetic fields to determine the output beam parameters and locations of particle losses.

INTRODUCTION

The drift-tube linac (DTL) structure, proposed by Alvarez in 1946, became the most popular type of low-energy proton linac for many decades. The DTL structure employs long cylindrical resonators (tanks) operating in the TM_{010} mode and containing a sequence of drift tubes (DTs) installed along the beam axis. DTL accelerators achieve their best efficiency for particle velocities from approximately 10% to 35% of the speed of light, i.e. $\beta = v/c = 0.1-0.35$. The Los Alamos Neutron Science Center (LANSCE) 201.25-MHz DTL covers a wide velocity range from $\beta = 0.04$ to 0.43, which corresponds to the proton energies from 750 keV to 100 MeV. The LANSCE DTL consists of four tanks. Some relevant parameters of the DTL tanks are listed in Table 1, where N_{DT} is the number of full DTs and N_{pc} is the number of post-couplers in the tank.

Table 1: LANSCE DTL Design Parameters [2]

Parameter	Tank 1	Tank 2	Tank 3	Tank 4
Energy in, MeV	0.75	5.39	41.33	72.72
β , in-out	0.04	0.107	0.287	.37-43
Length L , m	3.26	19.688	18.75	17.92
N_{DT}	30	65	37	29
N_{pc}	0	65	37	29
Aperture r_b , cm	0.75	1-1.5	1.5	1.5
Grad. E_0 , MV/m	1.6-2.3	2.4	2.4	2.5
Aver. ZT^2 , $M\Omega/m$	26.8	30.1	23.7	19.2

DTL TANK MODELS AND FIELDS

We have built 3D models of all four DTL tanks using CST Studio [3]. The EM fields in the tank models were calculated with CST MicroWave Studio (MWS), see [1, 4] for details. The CST model of tank 2 (T2) is shown in Fig. 1. This is the longest DTL tank (19.7 m) that contains 65 full DTs and two half-DTs on the end walls. The full DTs are supported by vertical stems. The tank cavity of radius 45 cm is shown in Fig. 1 as the blue-gray cylinder. Two upper insets in Fig. 1 show side views near the tank entrance (blue) and exit (green). The stabilizing post-couplers (gray) with rotating tabs can be seen in the end view of the tank in the right-bottom inset.

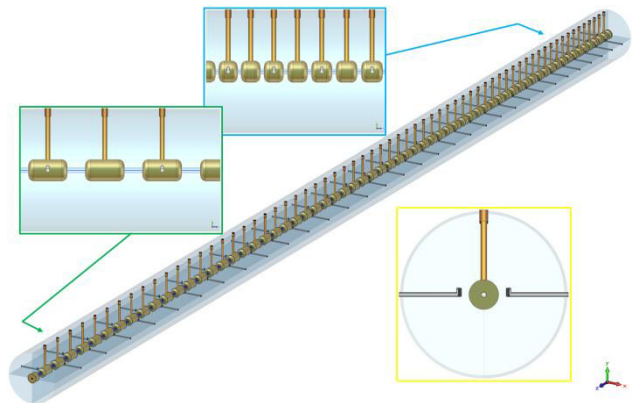


Figure 1: CST model of the LANSCE DTL tank 2. The cavity outer walls are removed for better view.

The shortest tank of the DTL, tank 1 (T1), does not have post-couplers, and its accelerating field is ramped: the average on-axis cell field E_0 increases along the tank from 1.6 to 2.3 MV/m. In T2-T4, the accelerating gradient E_0 is constant. Its flatness was tuned in the CST models by adjusting spacing between post-couplers and DTs, cf. [1, 4]. The RF fields in the tank models were calculated using primarily the MWS tetrahedral eigensolver. For accuracy, the meshes were refined locally, especially inside the DT apertures; details can be found in [4].

BEAM DYNAMICS

The MWS-calculated RF fields of the tuned operating mode in the tanks were used to study beam dynamics. The fields in the beam region were exported from MWS as text files in a format that can be imported into various multi-particle codes. We mainly use the CST Particle Studio (PS) particle-in-cell (PIC) solver. The static magnetic fields of the focusing quadrupoles, produced in Matlab as text files based on the hard-edge quad design values, were also imported into PS as external fields.

PIC Simulation Approach

We used two realistic initial particle distributions at the T1 entrance from PARMILA simulations (L. Rybarczyk). The first distribution (case A) started as 10K macro-particles (24-mA current) propagated through the future LANL RFQ [5] and following long beam transfer; 9587 particles (23 mA) reached the T1 entrance. The other distribution (case B) was traced from the Cockcroft-Walton (CW) injector through the existing transport lines that include a pre-buncher; 10K macro-particles at the entrance of tank 1 correspond to the 18-mA current into T1. At the T1 entrance the average beam energy $W = 0.75$ MeV; for case A (23 mA), the normalized rms horizontal emittance $\varepsilon_x = 0.29 \pi \mu\text{m}$ and vertical one $\varepsilon_y = 0.28 \pi \mu\text{m}$; for case B (CW 18 mA), $\varepsilon_x = 0.12 \pi \mu\text{m}$ and $\varepsilon_y = 0.10 \pi \mu\text{m}$. The same two distributions were used in [1], but there we traced only particles exiting T1 in a well-formed bunch, to speed up simulations in T2-T4, and ignored low-energy particles after the T1 exit, assuming that they will be lost anyway. This was sufficient to obtain DTL output beam parameters; essentially the same is done in many phase-space multi-particle codes, e.g. PARMILA [6]. Here we performed more detailed simulations that included tracking the low-energy tails, to study how they interact with the bunched beam and where the tail particles are lost.

We injected particles over 10 RF periods for each beam distribution described above. The PS PIC solver runs the input distribution through a tank with RF and quadrupole fields and records the particles in the exit plane. This exit distribution serves as an input for the next simulation, in a drift space between two tanks, then the next tank, and so on. To ensure the correct RF phases, $\varphi_s = -26^\circ$ in all tanks, the input distributions were time-delayed so that the bunch center reaches the middle of the first RF gap exactly at -26° . To reduce the mesh size for the PS runs, we cut the tank volume in the transverse directions x and y to just outside the DTs, but at the same time refined the mesh within the DT apertures [1]. Most beam parameters do not depend on the mesh size for PS runs with meshes from a few million to 56M mesh points in a tank model. The transverse emittances initially increase as the mesh size increases and then stay constant. The PS results presented here were obtained using meshes $\sim 35\text{M}$ points.

Simulation Results

Figure 2 shows the particle energy versus arrival time at the T1 exit for case B. Out of 100K injected particles, 85109 make it through T1: 80660 in 10 core bunches (top left) and 4449 with lower energies. Each blue dot corresponds to one macro-particle; many dots overlap in bunches, see the expanded view of the last bunch in the inset. In [1], we traced only one bunch and quoted the T1 transmission as 81%, while in fact additional 4.5% of injected particles exit T1 in the low-energy tail. These two components of the beam are separated in energy but still overlap in space. The average bunch energy is 5.36 MeV ($\beta = 0.106$) and that for the low-energy tail is 1.26 MeV ($\beta = 0.052$, i.e. about two times slower than the core

bunches). After the transition between T1 and T2, 80 more particles are lost, mostly from the tail. For comparison, in case A the total T1 transmission is 95.9% of the initial 95870 particles, with 94.1% (90235) in the 10 core bunches and only 1.75% (1675) in the tail.

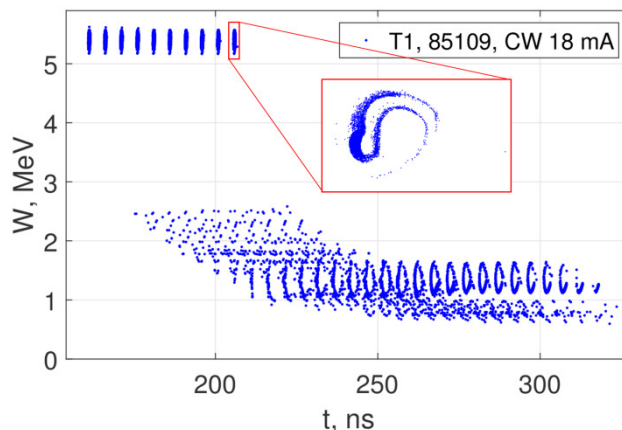


Figure 2: Energy of particles exiting DTL tank 1 versus time for case B (CW injection, 18 mA, 10 RF periods).

The LANSCE linac macro-pulses are much longer than the 10 RF periods (~ 50 ns) used in our simulations. This means that the following bunches, which are formed from RF periods injected later, will go through the low-energy tail left by the leading bunches. To take that into account to some extent, we modify the input distributions in T2-4 by shifting 10 bunches from the head of the distribution to its back so that they pass through the tail while moving in the tank. After that the time delay is adjusted for the center of the first bunch to arrive to the middle of the first RF gap at the right RF phase. The procedure is repeated after each tank. One example of such an “overlapped” input distribution into T3 for case A is shown in Fig. 3.

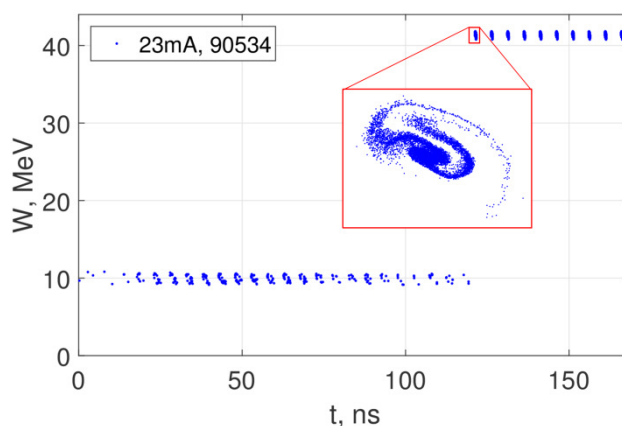


Figure 3: Particle energy in overlapped input for tank 3 versus delayed time for case A (23 mA, 10 RF periods).

In Fig. 3, out of 90534 particles in the distribution, 90235 are in 10 delayed bunches and only 299 are in the “tail”, which is now injected first. The first bunch contains 9024 particles; see the expanded view in the

Content from this work may be used under the terms of the CC BY 3.0 licence (© 2015). Any distribution of this work must maintain attribution to the author(s), title of the work, publisher, and DOI.

inset in Fig. 3. The ratio of average particle energy in bunches and the tail is close to 4. More exactly, the velocity ratio is $m = 2$: the average $\beta = 0.288$ in bunches and 0.144 in the tail. Similar patterns are observed after every tank though it is less obvious in Fig. 2 due to larger energy spread in the tail. This effect is not observed in phase-space codes (tail particles are too far in energy from synchronous ones and therefore usually discarded) but it has simple explanation. The tail particles that survive are accelerated with multiplicity $m = 2$: it takes them two RF periods to move from one RF gap to the next, while the main bunch particles are accelerated during every RF period ($m = 1$). Our PS simulations results for the beam transmission through the tanks for two distributions (A and B) are summarized in Table 2.

Table 2: Beam Transmission Fraction, %

	T1 out	T2 out	T3 out	T4 out
Case A, total	95.9	94.4	94.3	94.2
Case A, tail	1.75	0.31	0.24	0.10
Case B, total	85.1	82.5	81.6	81.4
Case B, tail	4.45	1.81	0.95	0.77

After bunches are formed in T1, practically all beam losses come from the low-energy tail (longitudinal halo). For the RFQ injection (case A), 94.1% of initial 23 mA is transmitted in bunches (100.16 MeV) and only 0.1% exits T4 in the longitudinal halo (~20 MeV). For C-W injection (case B), 80.7% of 18 mA is fully accelerated and 0.77% exits T4 as a 20-MeV halo. The difference is due to better bunching of the RFQ beam at the DTL entrance.

The emittance results are similar to those in [1]. The final normalized rms emittances after T4 for case A (23 mA) are $\epsilon_x = 0.44 \pi \mu\text{m}$ and $\epsilon_y = 0.38 \pi \mu\text{m}$; for case B (CW 18 mA), $\epsilon_x = 0.37 \pi \mu\text{m}$ and $\epsilon_y = 0.30 \pi \mu\text{m}$.

Particle Losses

Particle loss distributions inside the DTL tanks can be extracted from the PS results. The average power at 100% duty deposited by beam losses on DTs in T1 is compared for cases A and B in Fig. 4. The losses are larger in the downstream part of the tank. In T2 the beam losses are mainly on DTs 1-29 with smaller bore; in T3, the losses are mostly on the first 6 DTs [7]. The total average power at 100% duty deposited in each of the four DTL tanks by beam losses for the two cases is listed in Table 3. These values are small compared to the RF power losses on the DTs, which range from 60 kW in T1 to 833 kW in T4 [4].

Table 3: Average Power from Beam Losses, kW

	T1	T2	T3	T4
Case A (23 mA)	0.77	0.45	0.47	0.09
Case B (CW 18 mA)	1.72	0.74	1.66	0.55

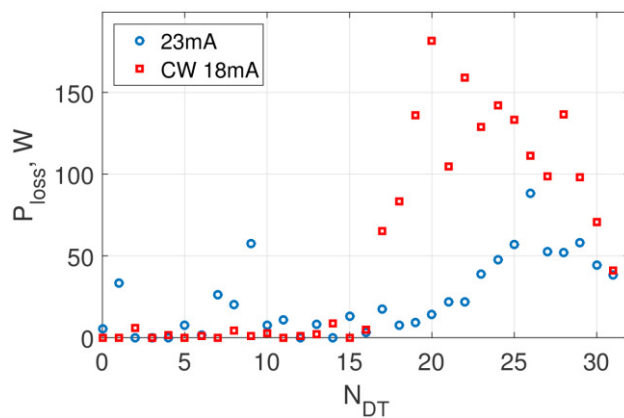


Figure 4: Average power deposited on DTs in tank 1 due to beam losses versus DT number.

CONCLUSION

We have developed 3D full-tank CST models of the 100-MeV LANSCE DTL. The RF fields of the operating mode in the tank models are calculated with MicroWave Studio. Particle Studio PIC simulations of beam dynamics allow us to elucidate interesting details of the longitudinal halo and particle loss in the DTL. More simulation results will be presented elsewhere [7]. As one can expect, the RFQ injection provides better transmission and lower losses compared to that from the existing Cockcroft-Walton injector. Our results indicate the presence of low-energy particles with energies around 20 MeV at the DTL exit. The low-energy tail amounts to about 0.8% of the regular 100-MeV beam with the existing injection scheme, and 0.1% for the future RFQ injection. We hope to verify this prediction experimentally.

ACKNOWLEDGMENT

The authors would like to thank R. Garnett, J. O'Hara, and L. Rybarcyk (LANL) for useful information and stimulating discussions.

REFERENCES

- [1] S.S. Kurennoy, "3D Mode Analysis of Full Tanks in Drift-Tube Linacs", Linac2014, Geneva, Switzerland, p. 300 (2014); <http://www.JACoW.org>
- [2] T.P. Wangler, *RF Linear Accelerators*, (Wiley-VCH, 2nd Ed., 2008), p. 95.
- [3] CST Studio Suite, CST, www.cst.com
- [4] S.S. Kurennoy, "RF Fields in LANSCE DTL Tanks", report AOT-HPE 14-005 (TN), Los Alamos, 2014; LA-UR-14-27599.
- [5] R.W. Garnett et al., "LANSCE H+ RFQ Project Status", THPF148, these proceedings, IPAC'15, Richmond, VA (2015).
- [6] Los Alamos Accelerator Code Group, laacg.lanl.gov
- [7] S.S. Kurennoy, "Particle Studio PIC Simulations of the LANSCE DTL", LANL report, in preparation.